RadioGraphics

MR Imaging of Endometriosis: Ten Imaging Pearls[1]

LEARNING OBJECTIVES FOR TEST 3

After completing this journal-based CME activity, participants will be able to:

■ List the different locations of solid endometriosis in the female pelvis.

■ Describe the typical MR imaging findings allowing differentiation of endometriomas from mature cystic teratomas and functional ovarian cysts.

■ Recognize MR imaging features of hematosalpinx, solid endometriosis, decidualized endometriosis, and malignant transformation of endometriosis.

TEACHING POINTS
See last page

Evan S. Siegelman, MD • Edward R. Oliver, MD, PhD

Endometriosis, which is defined as the presence of ectopic endometrial glands and stroma outside the uterus, is a common cause of pelvic pain and infertility, affecting as many as 10% of premenopausal women. Because its effects may be devastating, radiologists should be familiar with the various imaging manifestations of the disease, especially those that allow its differentiation from other pelvic lesions. The "pearls" offered here are observations culled from the authors' experience with the use of magnetic resonance (MR) imaging for the detection and characterization of pelvic endometriosis. First, the inclusion of T1-weighted fat-suppressed sequences is recommended for all MR examinations of the female pelvis because such sequences facilitate the detection of small endometriomas and aid in their differentiation from mature cystic teratomas. Second, it must be remembered that benign endometriomas, like many pelvic malignancies, may exhibit restricted diffusion. Although women with endometriosis are at risk for developing clear cell and endometrioid epithelial ovarian cancers (ie, endometriosis-associated ovarian cancers), imaging findings such as enhancing mural nodules should be confirmed before a diagnosis of ovarian malignancy is offered. The presence of a dilated fallopian tube, especially one containing hemorrhagic content, is often associated with pelvic endometriosis. Deep (solid infiltrating) endometriosis can involve the pelvic ligaments, anterior rectosigmoid colon, bladder, uterus, and cul-de-sac, as well as surgical scars; the lesions often have poorly defined margins and T2 signal hypointensity as a result of fibrosis. The presence of subcentimeter foci with T2 hyperintensity representing ectopic endometrial glands within these infiltrating fibrotic masses may help establish the diagnosis.

©RSNA, 2012 • *radiographics.rsna.org*

Introduction

Endometriosis is defined as the presence of endometrial tissue outside the uterus. This condition manifests in as many as 10% of women of reproductive age (1). Sampson (2) initially hypothesized that retrograde menstruation was the cause of endometriosis. However, the pathogenesis of endometriosis is complex and still debated (3). Retrograde menstruation is neither sufficient nor necessary for the development of endometriosis. Two other theories postulate that endometriosis develops from the metaplasia of pelvic peritoneal tissue and from the transformation of circulating stem cells (3). Several steps are required for the development of endometriosis (3). First, endometrial glands and stroma must migrate beyond the uterus. Second, the ectopic endometrial cells must attach to the peritoneum, extend into the mesothelium, and grow.

The reference standard for the diagnosis of pelvic endometriosis is laparoscopic biopsy of lesions with a suspicious appearance, followed by histologic confirmation (4). There are three forms of pelvic endometriosis (5,6). The first form is superficial peritoneal lesions, or noninvasive implants, which are well recognized at laparoscopy; these have been described as black, white, or red, depending on the degree of fibrosis, scarring, and hemorrhage within the lesion (7). Small nonhemorrhagic foci of superficial endometriosis are often not detectable with magnetic resonance (MR) imaging (8,9). The second form of pelvic endometriosis is ovarian endometrioma. The third form is deep (or solid infiltrating) pelvic endometriosis, which is defined by the invasion of endometrial glands and stroma at least 5 mm beneath the peritoneal surface. Of the three forms, deep pelvic endometriosis is thought to contribute most often to female pelvic pain and infertility, the two major manifestations

of endometriosis (6,10,11). Infertility is treated surgically (ie, removal of ovarian endometriomas and deep pelvic endometriosis and lysis of adhesions), with medical therapy, and with assisted reproduction techniques (10,11). Pain associated with endometriosis is initially treated with antiinflammatory agents and hormonal therapy (11). Depending on a woman's symptoms and desire to preserve fertility, surgical procedures may also be performed (1).

The article describes MR imaging appearances that may be helpful for differentiating endometriomas and deep pelvic endometriosis from other causes of pelvic pain and infertility in women. Instead of attempting a comprehensive review of MR imaging techniques and features, the authors offer 10 observations, or "pearls," based on their experience in the detection and characterization of pelvic endometriosis. This approach is designed to complement the coverage provided in previous *RadioGraphics* articles about MR imaging of endometriosis (12–20).

Pearl 1: Multiple T1-Hyperintense Adnexal Cysts Are Specific for Endometriomas

In 1991, Togashi and colleagues (21) showed that findings of an adnexal mass with high signal intensity on T1-weighted MR images and signal intensity lower than that of simple fluid on T2-weighted images helped establish a diagnosis of endometrioma with specificity greater than 90% (Fig 1). In addition to endometrioma, the main differential diagnoses of an adnexal lesion with high signal intensity on T1-weighted images include hemorrhagic functional ovarian cyst and mature cystic teratoma. In 1993, Outwater et al (9) compared the MR imaging features of endometriomas and hemorrhagic cysts and concluded that endometriomas tended to have higher T1 and lower T2 signal intensities than hemorrhagic cysts. The greater degree of T1 and T2 shortening

Figure 1. Left ovarian endometriomas, bilateral hematosalpinges, and fibrotic solid invasive endometriosis in the posterior uterus of a 47-year-old woman with severe pelvic pain. **(a)** Axial T1-weighted in-phase gradient-echo MR image shows two foci of high signal intensity in the left ovary (arrow) and multiple foci of high signal intensity in the left anterior and midline posterior pelvis (arrowheads). **(b)** Axial opposed-phase T1-weighted fat-suppressed gradient-echo MR image shows persistent high signal intensity in all three regions, a finding that helps exclude the presence of a fat-containing mature cystic teratoma. The improved dynamic range achieved with fat suppression facilitates visualization of a subcentimeter endometrioma of the anterior left ovary (arrow). **(c)** Axial T2-weighted fast spin-echo MR image shows low signal intensity within the left ovarian endometriomas (solid arrow) and lesser degrees of T2 signal hypointensity within the dependent portions of the loculi in the left anterior and midline posterior pelvis (arrowheads). The posterior uterus is markedly thickened with low-signal-intensity soft tissue *(F)* containing scattered 2–4-mm foci of high signal intensity (open arrows). Although the tissue has the appearance of adenomyosis, it is separated from the posterior junctional zone *(JZ)*. These findings are suggestive of fibrotic endometriosis. **(d, e)** Sagittal **(d)** and coronal fat-suppressed **(e)** T2-weighted MR images show dilatation of the right and left fallopian tubes, respectively (arrows). In **d**, extension of fibrotic endometriosis *(F)* into the posterior uterus is seen. The patient later underwent hysterectomy and bilateral salpingo-oophorectomy, at which the MR imaging findings were confirmed.
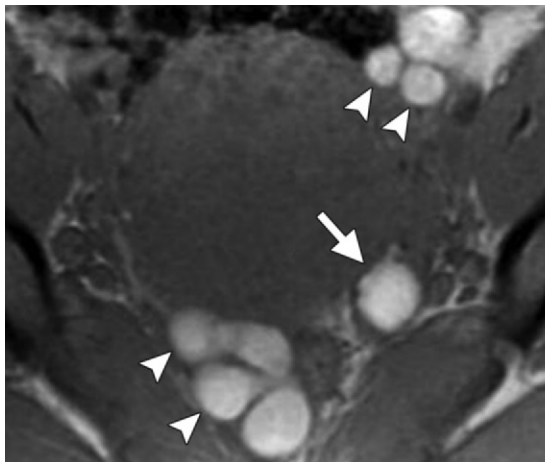
a.
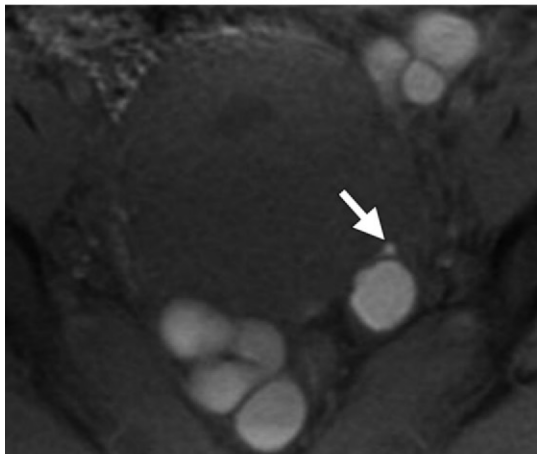
b.
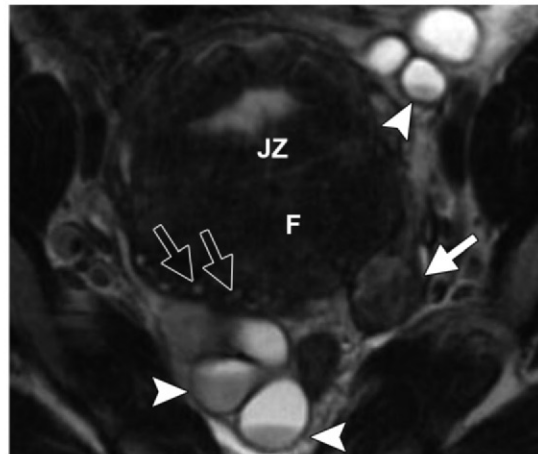
c.
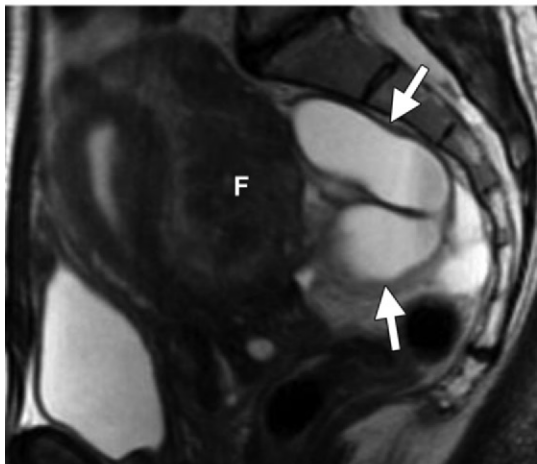
d.
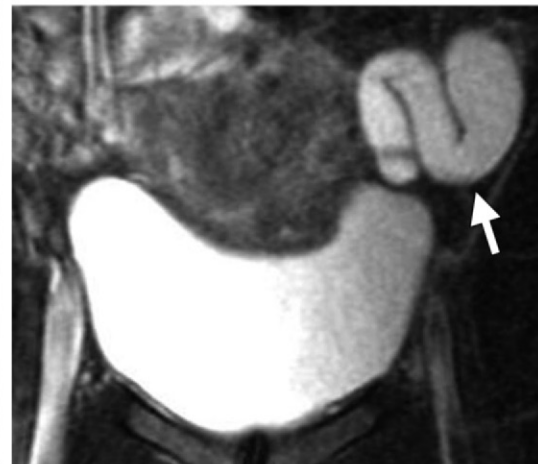
e.

in endometriomas is attributable to their higher protein concentration and viscosity. The lower T2 signal intensity of endometriomas compared with that of functional, or simple, ovarian cysts has been described as "T2 shading" (22). Bilaterality and multifocality of adnexal lesions, along with the other characteristics discussed and illustrated in the following sections, can help help establish a diagnosis of endometrioma with even greater specificity than T1 signal hyperintensity alone.

RadioGraphics
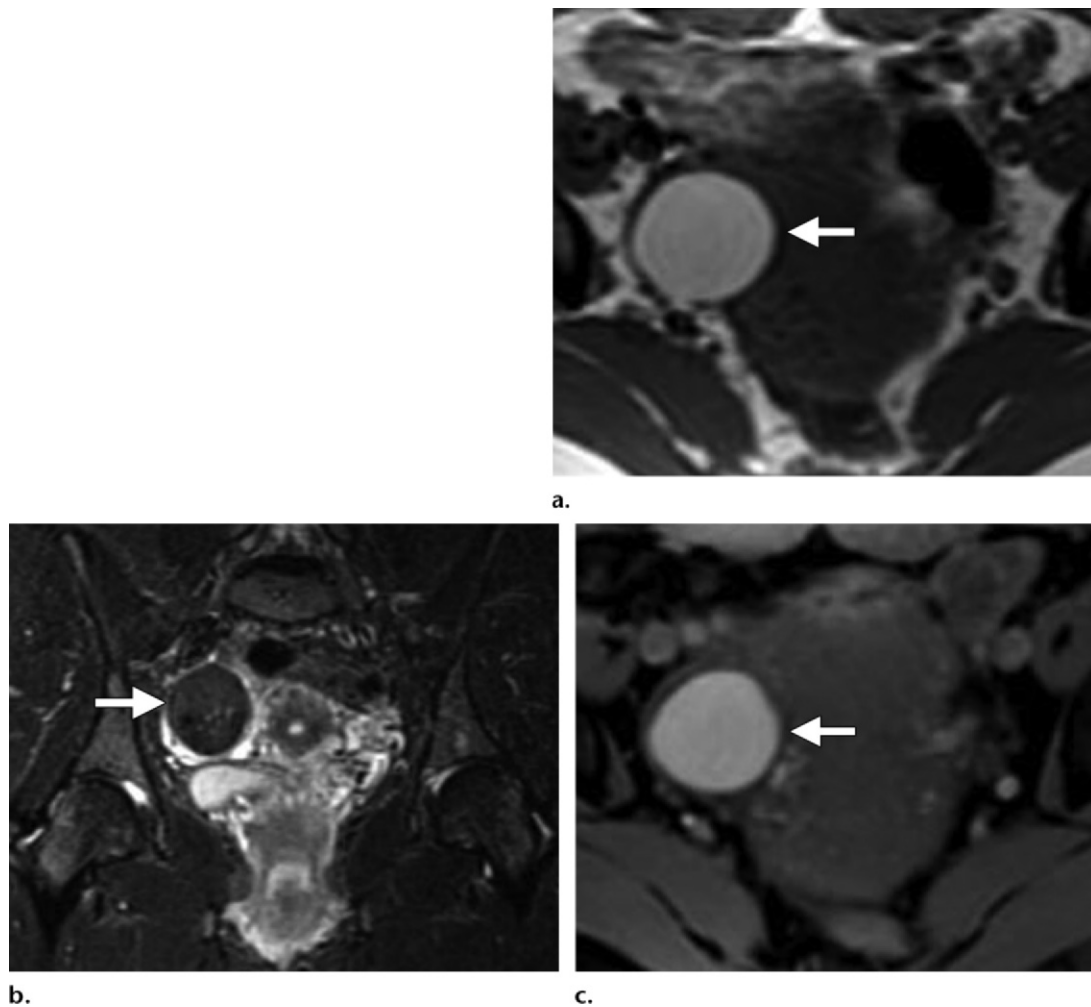
Figure 2. Right ovarian endometrioma in a 35-year-old woman that might have been misinterpreted as a mature cystic teratoma with reliance on short inversion time inversion-recovery (STIR) imaging alone to detect intralesional fat. **(a)** Axial T1-weighted spin-echo MR image shows a high-signal-intensity mass (arrow) within the right adnexa. **(b)** Coronal STIR MR image shows that the mass (arrow) has low signal intensity similar to that of suppressed fat. **(c)** Axial fat-suppressed gradient-echo MR image shows high signal intensity of the mass (arrow), a finding that helps confirm that it is not composed of fat. The low signal intensity of the mass on the STIR image could be secondary to either T1- or T2-shortening effects but cannot be considered indicative of fat content. To avoid this pitfall of STIR MR imaging of the female pelvis, MR systems capable of performing chemical-shift fat suppression should be used.

Pearl 2: Female Pelvis MR Imaging Protocols Should Include T1-weighted Fat-suppressed Sequences

Although T1-weighted fat-suppressed imaging was not performed in the landmark studies by Outwater et al (9) and Togashi et al (21), we recommend that all MR imaging examinations of the female pelvis include a T1-weighted fat-suppressed sequence for two reasons: First, the loss of signal intensity within a T1-hyperintense adnexal mass at fat-suppressed imaging facilitates characterization of the mass as a mature cystic teratoma (23–27). Second, saturation of the high signal intensity of fat improves the dynamic range of T1-weighted images by enhancing the differences among non–fat-containing T1-hyperintense structures, thereby enabling more sensitive detection of smaller endometriomas (Figs 1b, 2c, 3b).

Teaching Point

a.

b.   c.
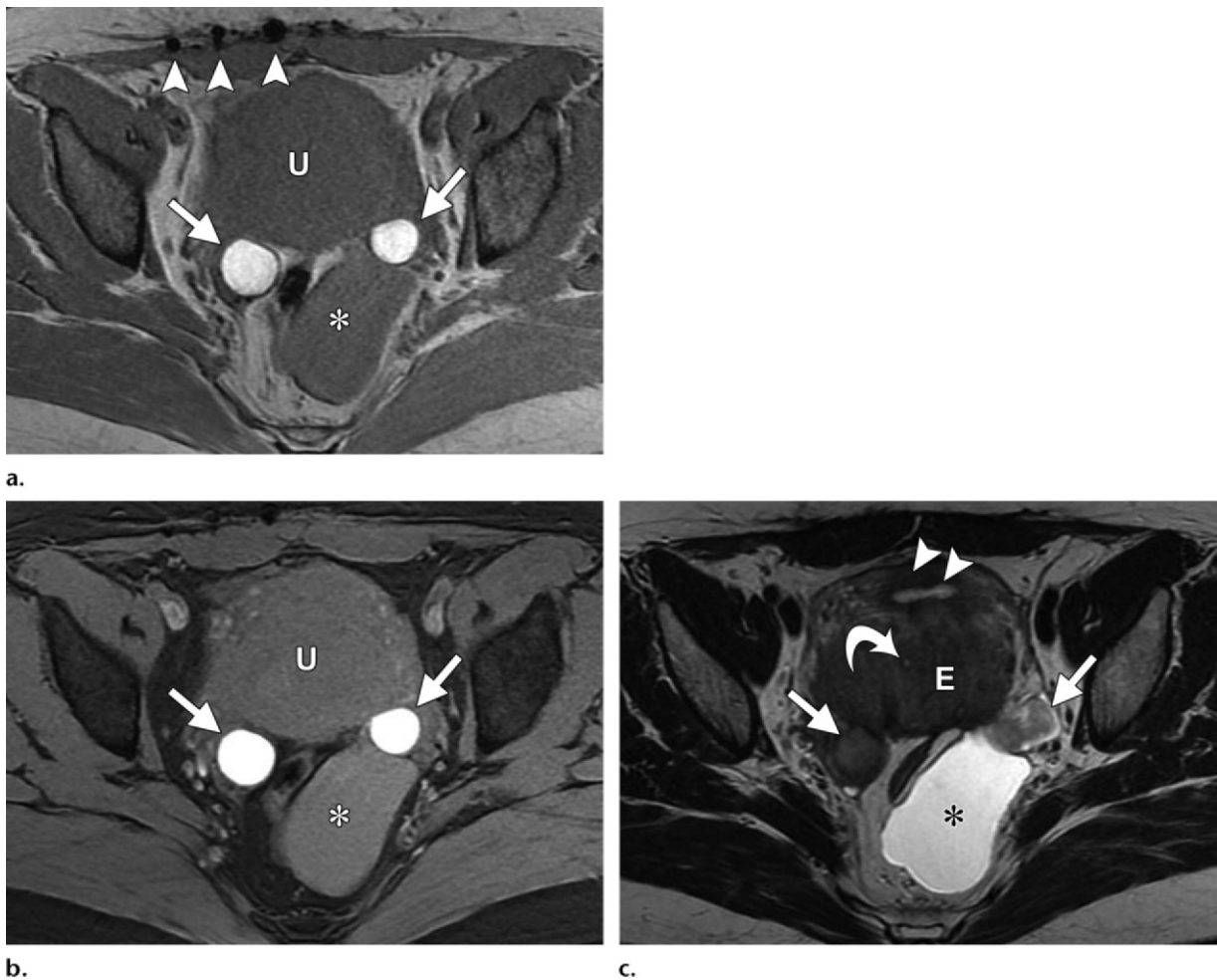
Figure 3.   Bilateral endometriomas, solid endometriosis of the posterior uterus, and left-sided peritoneal inclusion cyst in a 43-year-old woman. **(a, b)** Axial T1-weighted in-phase **(a)** and fat-suppressed opposed-phase **(b)** gradient-echo MR images show bilateral hyperintense adnexal lesions (arrows) that retain high signal intensity with fat suppression. A peritoneal inclusion cyst (∗) is also shown posterior to the uterus *(U)*. Susceptibility artifacts anterior to the rectus muscles (arrowheads in **a**) indicate that the patient has undergone a previous surgical procedure. **(c)** Axial T2-weighted MR image shows shading within the bilateral endometriomas (straight arrows). The normal endometrial complex and junctional zone are shown in the anterior uterus (arrowheads). The posterior uterus is markedly enlarged by poorly marginated soft tissue *(E)* with low T2 signal intensity and scattered internal 1–2-mm foci of higher signal intensity (curved arrow) representing infiltration of solid endometriosis into the uterine wall. Loculated fluid posterior to the left ovary represents the peritoneal inclusion cyst (∗).

Pearl 3: Low Signal Intensity of Adnexal Masses on STIR MR Images Is Not Specific for Mature Cystic Teratoma and Does Not Exclude Endometrioma

Frequency-selective fat suppression cannot be performed with some low-field-strength MR imaging systems that lack enhanced gradients (28). These systems can eliminate the signal intensity from fat only with the use of STIR techniques. It is worth repeating the admonition of Krinsky et al (29) that the loss of T1 signal hyperintensity on STIR images is not a finding specific to fat; hemorrhagic ovarian cysts and endometriomas can have T1 relaxation times similar to that of fat (ie, they can show "suppressed" signal intensity) and thus may mimic mature cystic teratomas at STIR imaging (Fig 2b). Use of an MR imaging system capable of chemically selective T1-weighted fat-suppressed imaging will prevent the occurrence of this pitfall.

Pearl 4: Benign Endometri-omas Show Restricted Diffusion

Diffusion-weighted imaging with quantitative assessment of apparent diffusion coefficient (ADC) values has been incorporated into pelvic MR imaging protocols (30). The reader is referred to previous *RadioGraphics* articles for reviews of the principles of diffusion-weighted imaging and ADC calculation and their application at imaging of the female pelvis (31,32). The presence of restricted diffusion and low ADC values within an adnexal lesion does not have a high positive predictive value or specificity for the diagnosis of malignancy. Benign hemorrhagic ovarian cysts (33), endometriomas, and solid endometrial implants (34), as well as benign mature cystic teratomas (35), also demonstrate restricted diffusion (Fig 4). Endometriomas have low ADC values in part because of "T2 blackout effects" (36,37). On a diffusion-weighted image obtained with a low b value (which is a type of T2-weighted fat-suppressed image), an endometrioma exhibits low signal intensity resembling the T2 shading discussed in the section on "Pearl 1." Thus, endometriomas have less signal intensity to lose on images obtained with higher b values than adnexal masses with higher T2 signal intensity do. Because the ADC value is based on the slope of the signal intensity loss between acquisitions at low b values and those at higher b values, endometriomas often have low ADC values. In a study evaluating both endometriomas and solid endometrial implants, Busard and colleagues (34) showed a significant correlation between the T2 signal intensity ratio (ie, the signal intensity of the endometriomas or implants divided by the signal intensity of muscle) and the ADC value.

## Pearl 5: Hemato-salpinx Should Be Considered Specific for Pelvic Endometriosis

The most common cause of a dilated fallopian tube encountered at pelvic imaging is pelvic inflammatory disease (18,20). In acute pelvic inflammatory disease, a dilated fallopian tube is usually a pyosalpinx. In the chronic form of the disease, a hydrosalpinx develops secondary to adhesions and scarring. Dilated fallopian tubes secondary to pelvic inflammatory disease do not exhibit T1 shortening at MR imaging (38). Endometriosis is another frequent cause of dilated fallopian tubes, with 30% of women with the disease demonstrating tubal involvement at laparoscopy (20,39). The presence of T1-weighted hyperintensity within a dilated fallopian tube is suggestive of endometriosis (Fig 1) and may be the only finding at MR imaging in some women (38). In women with endometriosis and a dilated fallopian tube, approximately 40% of the tubes had T1-hyperintense contents, whereas 60% had imaging features suggestive of a simple hydrosalpinx (38). Low T2 signal intensity (T2 shading) (Fig 1c–1e) is not often present within a hematosalpinx that occurs in association with endometriosis (38,40). T2 shading may be absent in these cases because women with endometriosis develop dilated fallopian tubes secondary to endometrial implants on the serosal surface of the tubes, as opposed to implants within the tubes (20). Recurrent hemorrhage within the serosal implants presumably leads to the formation of peritubal adhesions and subsequent tubal obstruction.

Teaching Point

Pearl 6: Obstruction of Antegrade Menstrual Flow Increases the Risk for Endometriosis

Although most women have reflux menstruation, only 5%–10% of them develop endometriosis (6,10). However, a subset of women with müllerian duct anomalies that cause obstruction of antegrade menstruation are considered to have an increased risk for endometriosis (6,40–42). This subset includes women who have a unicornuate uterus with a noncommunicating rudimentary horn or uterus didelphys with a transverse vaginal septum. MR imaging is an ideal modality for evaluating primary amenorrhea in girls (43) as well as suspected uterine anomalies in women (44,45). If there is an obstruction, MR imaging can be used to localize it, determine which segments of the reproductive tract are distended with blood, and determine whether endometriomas and other manifestations of endometriosis are present (Fig 5).
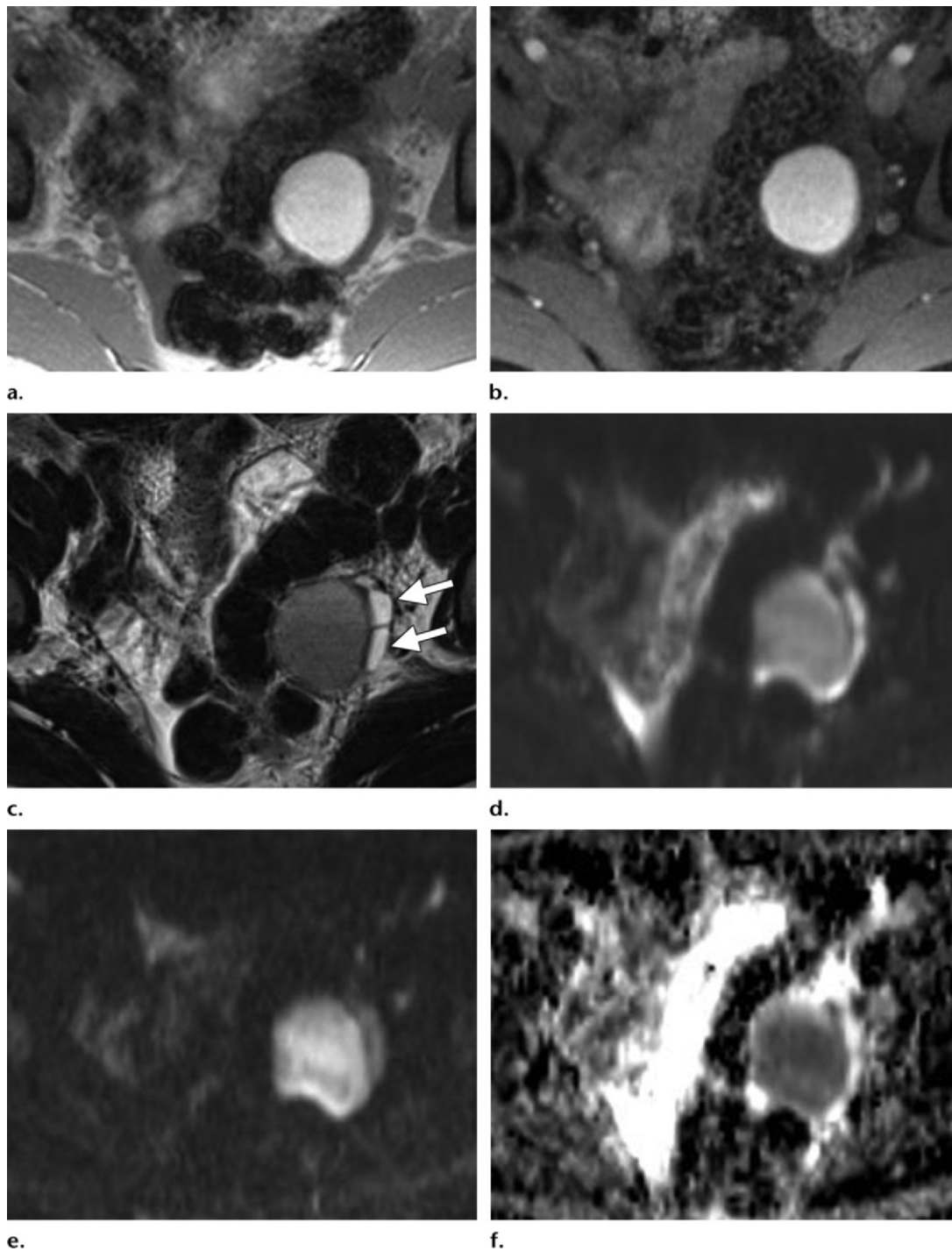
Figure 4.   Endometrioma of the left ovary in a 33-year-old woman. **(a, b)** Axial T1-weighted in-phase **(a)** and opposed-phase fat-suppressed **(b)** gradient-echo MR images show a T1-hyperintense left ovarian lesion, a feature suggestive of endometrioma. **(c)** Axial T2-weighted MR image shows lower signal intensity in the endometrioma than in the adjacent normal ovarian follicles (arrows). **(d, e)** Diffusion-weighted MR images obtained with *b* values of 50 **(d)** and 800 **(e)** sec/mm^2 show low to intermediate signal intensity in both the endometrioma and the normal follicles. **(f)** ADC map from diffusion-weighted MR imaging shows restricted diffusion in the endometrioma relative to that in the adjacent ovarian follicles.
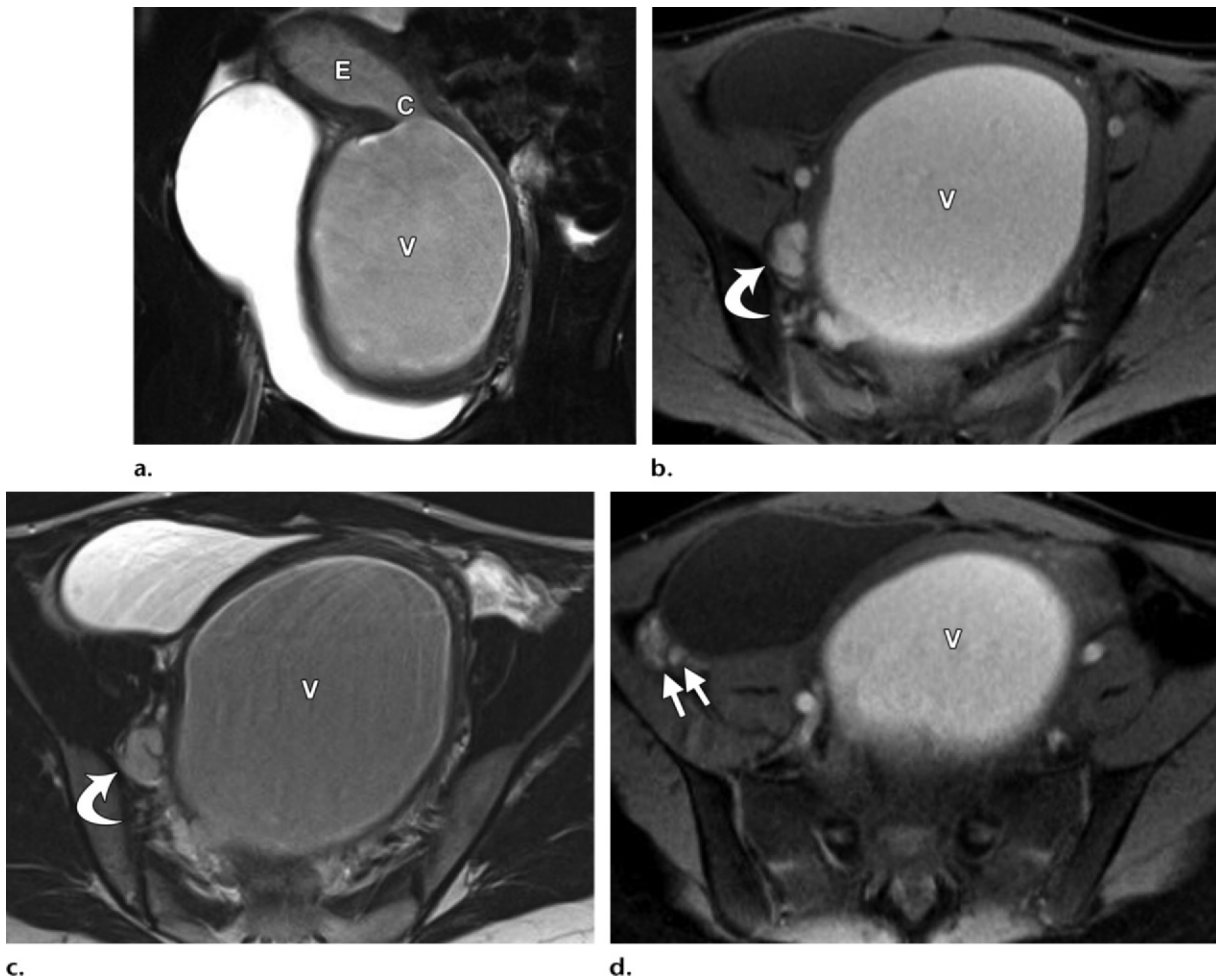
Figure 5. Hematometrocolpos, hematosalpinx, and endometriomas in a 15-year-old girl with an obstructing transverse vaginal septum. **(a)** Coronal T2-weighted fat-suppressed MR image shows dilatation of the endometrium *(E)*, endocervix *(C)*, and proximal vagina *(V)* due to a transverse vaginal septum (not shown). **(b, c)** Axial T1-weighted fat-suppressed **(b)** and T2-weighted fast spin-echo **(c)** MR images obtained at the level of the uterus show the distended vaginal canal *(V)* and segments of a dilated right fallopian tube (arrow). These structures have similar high T1 signal intensity and intermediate T2 signal intensity. **(d)** Axial T1-weighted fat-suppressed MR image obtained at the level of the right ovary shows multiple subcentimeter high-signal-intensity endometriomas (arrows), findings confirmed at resection of the vaginal septum.

Pearl 7: Decidualized Endometriosis May Mimic Ovarian Malignancy in Pregnant Women

During pregnancy, increased progesterone levels promote hypertrophy of the endometrial stromal cells and formation of the vascular decidual lining of the uterus. Endometrial stromal cells within endometriomas may also respond to the hormonal changes of pregnancy by forming vascular mural nodules. Decidualized endometriosis has been described as a mimic of ovarian cancer at ultrasonography (US) and MR imaging (46–50). An MR imaging feature that may be specific for decidualized endometriosis is the T2 signal hyperintensity of the mural nodules, which are isointense relative to the thickened decidualized endometrium (Fig 6). Decidualized endometriosis can be managed conservatively and surgical procedures avoided. After childbirth or termination of a pregnancy, decidualized endometriosis has been reported to either resolve or regress to uncomplicated endometriomas (51,52).

Teaching Point
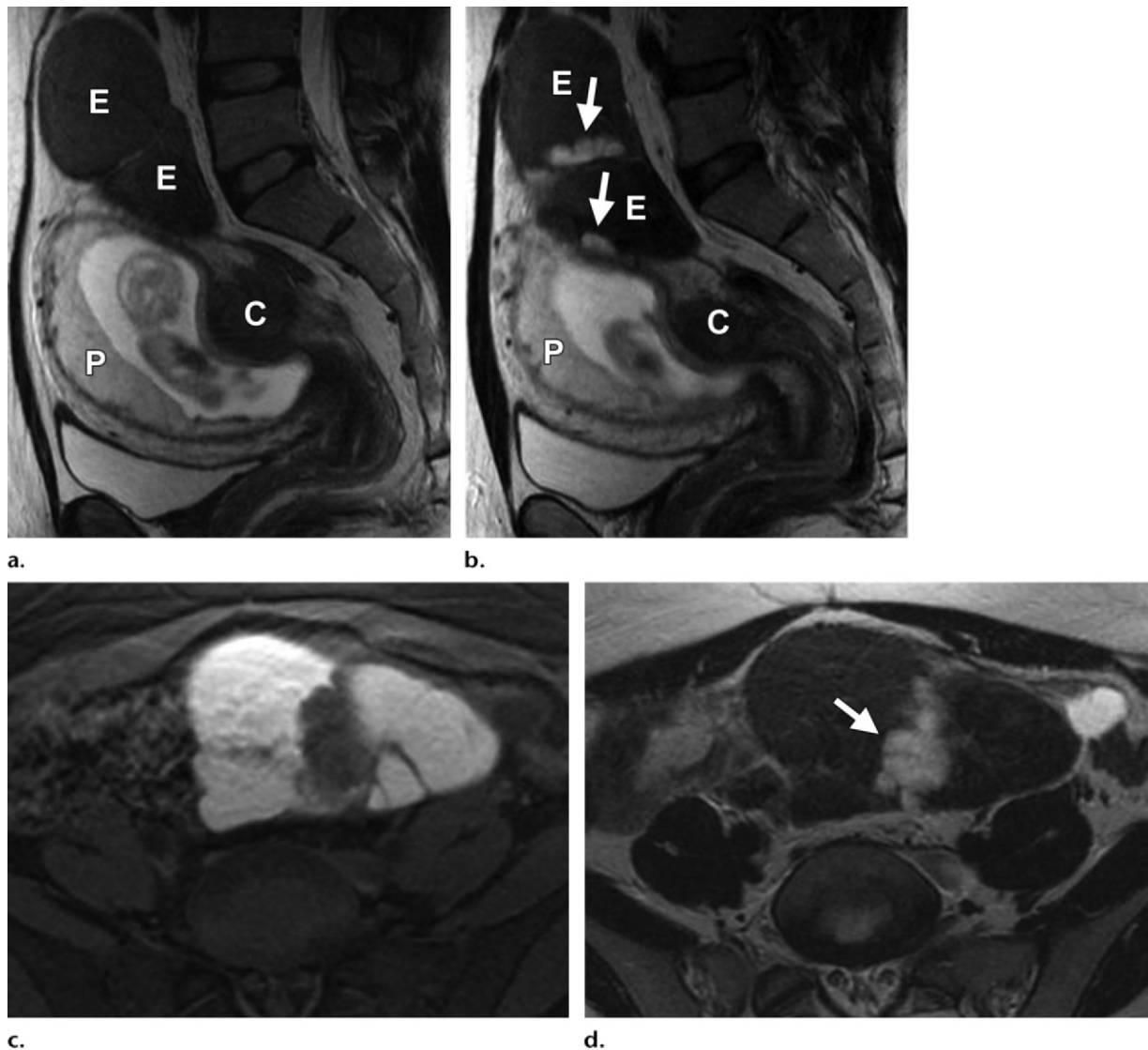
Figure 6.   Decidualized endometriosis in a 36-year-old woman in the 12th week of pregnancy. **(a, b)** Sagittal T2-weighted fast spin-echo MR images show an intrauterine gestational sac, a focal contraction *(C)* of the posterior myometrium, and an anterior placenta *(P)*. The bilobed low-signal-intensity mass above the uterus represents an endometrioma *(E)*. Mural nodules with higher signal intensity within the endometrioma (arrows in **b**) represent decidualized endometriosis. **(c, d)** Axial T1-weighted fat-suppressed **(c)** and T2-weighted fast spin-echo **(d)** MR images show the typical signal intensity of an endometrioma, with T1 hyperintensity and T2 shading, and the higher T2 signal intensity of decidualized endometriosis (arrow in **d**).

Pearl 8: Endometriomas Can Transform into Clear Cell or Endometrioid Epithelial Ovarian Carcinomas

Women with endometriosis are at risk for developing both clear cell and endometrioid subtypes of epithelial ovarian cancer (53). An estimated 2.5% of women with endometriosis develop ovarian cancer. Women with endometriosis-associated ovarian cancer have a better prognosis than woman with ovarian cancer but no endometriosis, because women in the former group tend to develop lower grade tumors that manifest at an earlier stage (54,55). Endometriosis is one of several benign causes of an abnormal

CA-125 level (56); thus, an elevated biomarker value in isolation is not specific for endometriosis-associated ovarian cancer. In contrast, the human epididymal secretory protein E4 level is elevated in women with either endometriosis-associated or conventional ovarian cancer, but not in women with benign endometriosis (57,58).

MR imaging features that are suggestive of malignant endometriomas have been described elsewhere (15,40,59,60). Those features include increases in the size and T2-weighted signal intensity of an endometrioma (Fig 7a). A more specific finding of malignant transformation of an endometrioma is the development of enhancing mural nodules (Fig 7b–7f).

Pearl 9: Solid Fibrotic Masses of Endometriosis Are Common and Easily Overlooked

Although most endometriomas are easily recognized on the basis of their T1 hyperintensity, solid masses of endometriosis can easily be overlooked. Part of the challenge in their recognition is due to the fact that solid endometriosis has low T2 signal intensity and may be located adjacent to normal T2-hypointense structures (62). Solid endometriosis, which also is referred to as deep pelvic endometriosis (12) or deeply infiltrative endometriosis (5,17), is defined by the extension of endometrial glands and stroma at least 5 mm beneath the peritoneal surface (5,63). Unlike endometriomas, which contain viscous proteinaceous and hemorrhagic contents, solid masses of endometriosis are composed of ectopic endometrial gland and stromal cells embedded within dense fibrous tissue and smooth muscle. The typical appearance of solid endometriosis can be appreciated by looking at adenomyosis, also known as endometriosis interna. At MR imaging, uterine adenomyosis appears as poorly marginated tissue with low T2 signal intensity and variable internal

1–4-mm foci with high T2 signal intensity (64). The former represents hypertrophied smooth muscle and fibrous tissue, and the latter represent ectopic endometrial glands. Visualization of the ectopic endometrial glands varies, depending on their location and the patient's immune response. Unlike ovarian endometriomas, fibrotic masses are less likely to contain high T1 signal intensity, perhaps because surrounding fibrosis and smooth muscle hypertrophy minimize cyclical bleeding within the ectopic endometrial glands.

Coutinho and colleagues (12) divided the anatomic locations of solid endometriosis lesions into anterior, middle, and posterior compartments of the pelvis, placing the anterior rectosigmoid colon and the uterosacral ligaments in the posterior compartment and the round ligaments and bladder in the anterior compartment. Women with a uterus in anteflexion are more likely to develop solid endometriosis of the anterior compartment, whereas those with a uterus in retroflexion are more likely to develop posterior compartment endometriosis (65). These findings support the hypothesis advanced by Sampson (2), that retrograde menstruation contributes to the early pathogenesis of endometriosis.

The next five sections describe common locations of solid endometriosis in the anterior and posterior compartments of the pelvis.

Uterosacral Ligaments

The uterosacral ligaments are considered the most common location of solid endometriosis (63). Affected women may present with pelvic pain, including dyspareunia. Routine MR imaging has a reported sensitivity of 69% and a specificity of more than 90% for the diagnosis of uterosacral ligament endometriosis (66); in one study, it was more accurate than either endovaginal US or endorectal US (67) (Fig 8). When women undergo MR imaging for suspected deep pelvic endometriosis, some investigators advocate distention of the vagina, rectum, or both with sterile gel to obtain better definition of the posterior cul-de-sac, the anterior rectosigmoid colon, and the uterosacral ligaments (12,17,68–70).
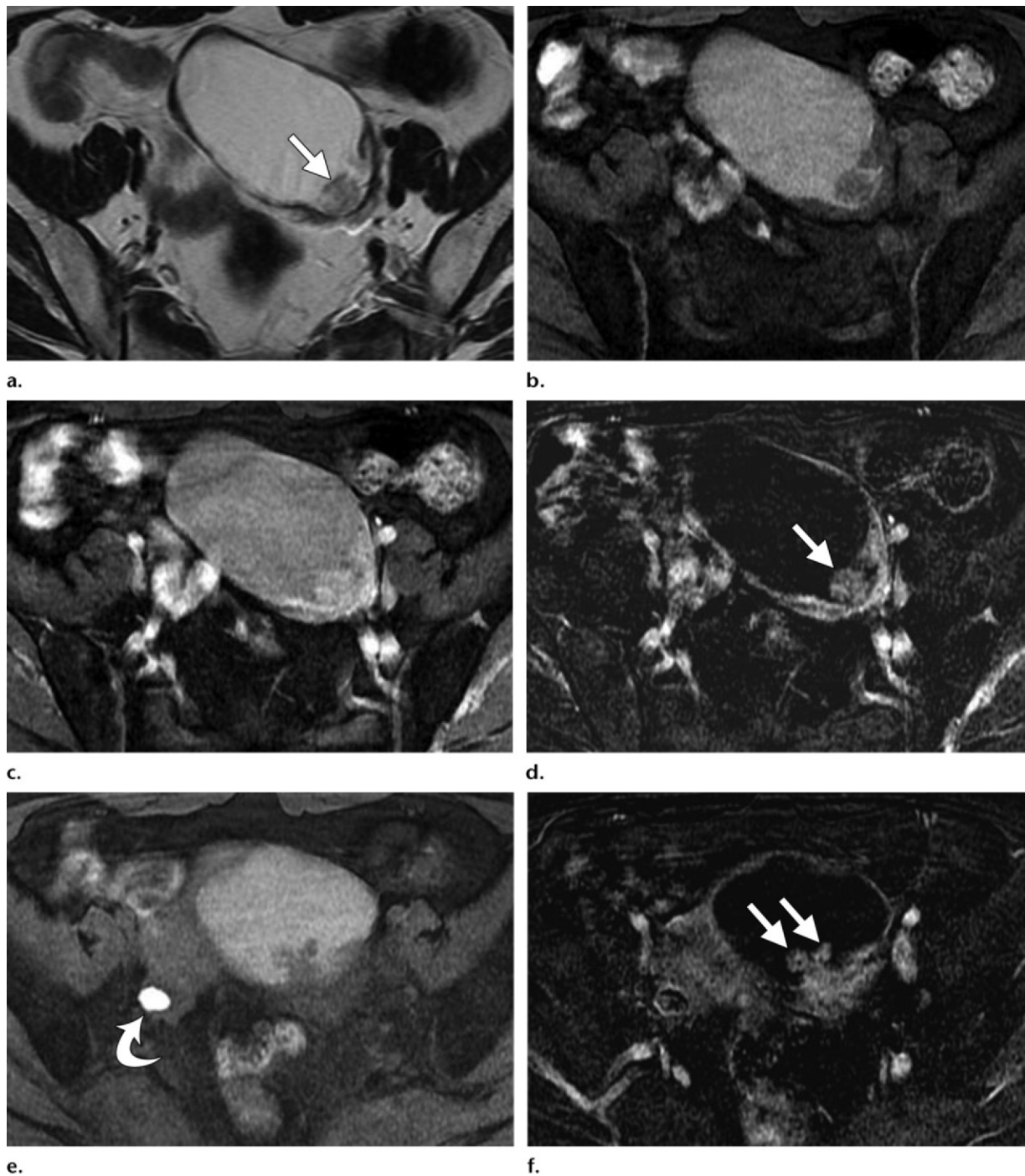
Figure 7. Endometrioid cystadenocarcinoma of the left ovary in a 51-year-old woman with long-standing endometriosis. **(a)** Axial T2-weighted MR image shows a cystic pelvic mass that also contains solid soft tissue (arrow). The signal of the cystic component was slightly hypointense to that of the bladder (not shown). **(b, c)** Axial T1-weighted fat-suppressed gradient-echo MR images obtained before **(b)** and after **(c)** the administration of a gadolinium-based contrast material show that the cystic component has T1 hyperintensity, a finding suggestive of proteinaceous or hemorrhagic content. The signal intensity of the solid component of the mass, relative to that of the cystic portion, is lower in **b** and higher in **c**. **(d)** MR image obtained by subtracting the unenhanced image dataset from the contrast-enhanced image dataset facilitates the detection of enhancing tissue (arrow) by increasing the dynamic range (61) and eliminating the high signal intensity of nonenhancing hemorrhagic and proteinaceous tissue. **(e, f)** Unenhanced T1-weighted fat-suppressed **(e)** and gadolinium-enhanced subtraction **(f)** MR images obtained at a lower level show additional enhancing nodular components (arrows in **f**) in the tumor. A 1-cm right ovarian endometrioma (arrow in **e**) is also seen.
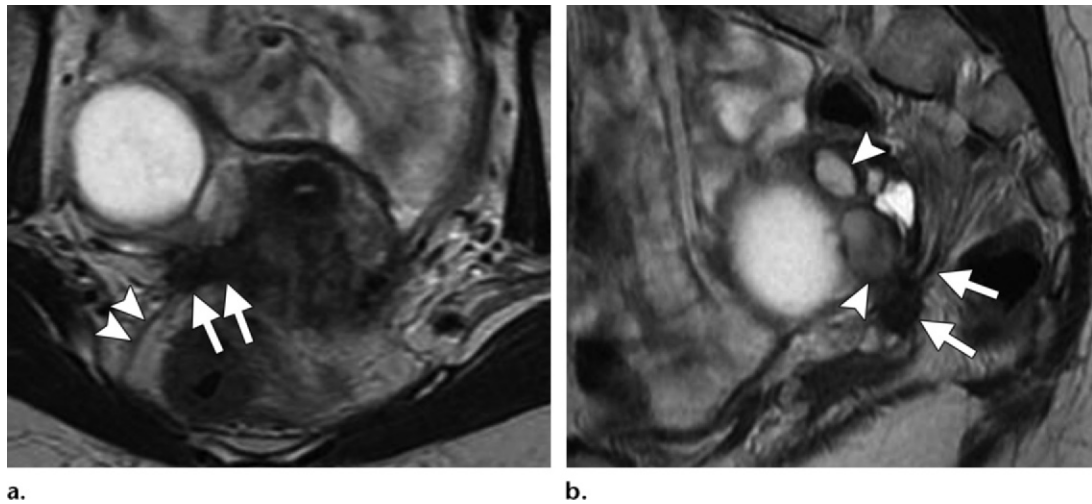
Figure 8. Solid fibrotic thickening of the uterosacral ligament in a 40-year-old woman with endometriosis and pelvic pain. **(a)** Axial T2-weighted MR image shows low-signal-intensity, masslike thickening of the proximal right uterosacral ligament (arrows). The normal-appearing sacral portion of the ligament (arrowheads) is also depicted. **(b)** Sagittal T2-weighted MR image shows bandlike fibrotic adhesions above the ligament (arrows) and shading within the superior right ovarian endometriomas (arrowheads).
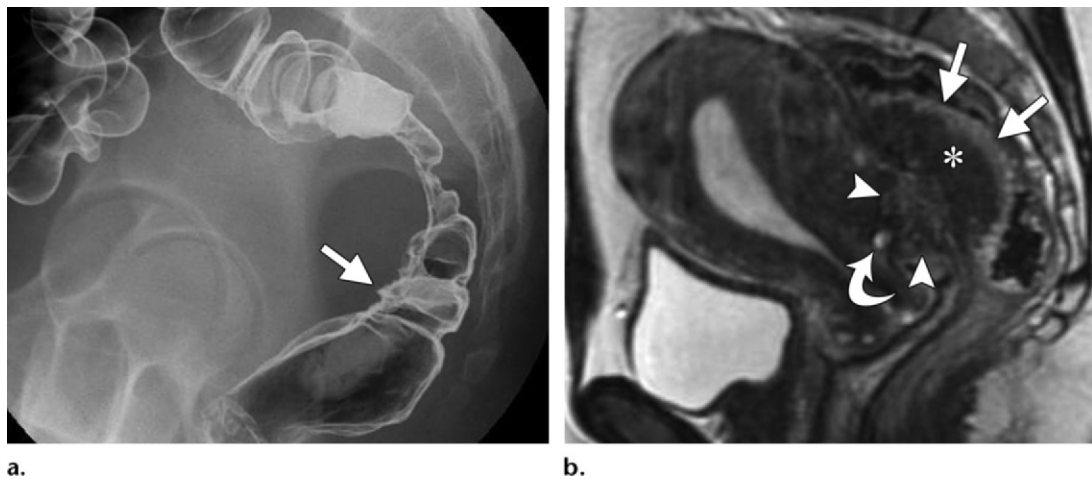

Figure 9. Solid invasive endometriosis of the rectosigmoid colon in a 40-year-old woman. **(a)** Lateral image from a double-contrast barium examination shows circumferential narrowing of the rectosigmoid colon, with mass effect, spiculation, and pleating of the anterior margin (arrow). **(b)** Sagittal T2-weighted fast spin-echo MR image shows extraluminal findings suggestive of solid invasive endometriosis. The mushroom cap sign represents the low-signal-intensity core of fibrotic endometriosis and hypertrophic muscularis propria (∗) capped by high-signal-intensity mucosa (straight arrows). Invasion of the serosal surface of the uterus and obliteration of the cul-de-sac (arrowheads) are seen, with high-signal-intensity 1–3-mm foci (curved arrow) representing ectopic endometrial glands.

Anterior Rectosigmoid Colon

The rectosigmoid colon is the intestinal segment most commonly involved in endometriosis. Women with symptoms specific for rectosigmoid involvement often benefit from resection of serosa-based lesions (71). When there is deep invasion of the muscularis propria, complete surgical resection of the affected bowel segment may be performed (72). At surgical resection, most endometrial lesions that have penetrated the muscularis propria and invaded the submucosa are found to involve at least 40% of the circumference of the rectal wall (73). The MR imaging features of solid rectosigmoid endometriosis have been well described and include a "mushroom cap" sign, which is considered a specific finding of solid invasive endometriosis of the rectosigmoid colon on T2-weighted MR
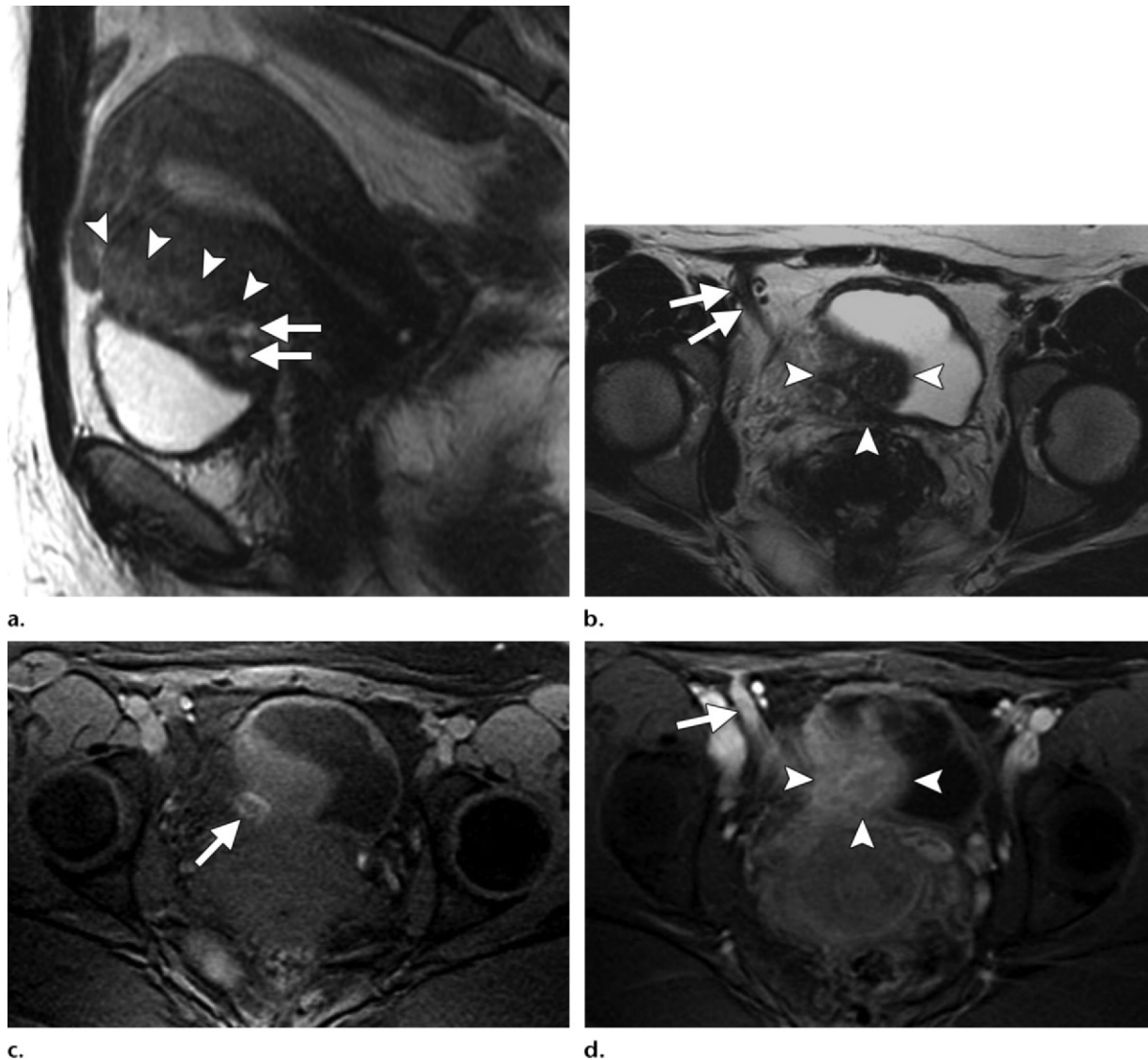
Figure 10.   Solid endometriosis of the bladder and right round ligament in a 40-year-old woman. **(a, b)** Sagittal **(a)** and axial **(b)** T2-weighted MR images show a poorly marginated, low-signal-intensity mass (arrowheads) in the right posterior bladder wall that extends posteriorly, obliterating the vesicouterine pouch. Intralesional 1–4-mm high-signal-intensity foci (arrows in **a**) represent ectopic endometrial glands. The right round ligament is thickened (arrows in **b**) as it courses inferiorly toward the canal of Nuck. **(c, d)** Axial T1-weighted gradient-echo fat-suppressed MR images obtained before **(c)** and after **(d)** the administration of a gadolinium-based contrast material show T1 hyperintensity in some of the endometrial glands within the posterior bladder lesion (arrow in **c**) and solid enhancement of both the bladder mass (arrowheads in **d**) and the thickened round ligament (arrow in **d**).

images (74). The low-signal-intensity base of the mushroom is attributed to hypertrophy and fibrosis of the muscularis propria, whereas the high-signal-intensity cap represents the mucosa and submucosa, which are displaced into the bowel lumen (Fig 9).

Bladder

When endometriosis involves the urinary tract, the bladder (especially the posterior wall) is frequently affected. In one case series involving 20 women who underwent surgical resection of blad-

der endometriosis, 19 had disease of the posterior bladder wall with direct extension that either partially or completely obliterated the vesicouterine pouch (also known as the anterior cul-de-sac) (75) (Fig 10). Patients with endometriosis involving the bladder usually present with nonspecific symptoms such as dysuria. Cyclical hematuria is less common and, when present, is suggestive of extension of endometriosis through the detrusor muscle, with mucosal involvement (76). At MR

imaging, solid endometriosis of the bladder appears similar to other solid endometriotic masses described in this article, specifically, as poorly defined infiltrative or nodular lesions with low T2 signal intensity, centered within the vesicouterine pouch, and including internal foci with variable T1 and high T2 signal intensity representing ectopic glandular tissue (12,77).

Round Ligaments

Women with symptomatic deep endometriosis of the round ligament usually present when there is involvement of the distal ligament in the canal of Nuck. A painful inguinal mass, with or without menstrual cycle–related variations in size or severity of symptoms, is the typical clinical manifestation (78–82). Reports concerning specific symptoms associated with endometriosis of the central, intrapelvic part of the round ligament are limited. In a study of 174 women who underwent laparoscopy for treatment of solid invasive endometriosis, the prevalence of disease in the intrapelvic segment of the round ligament was 15% (83). Similar to solid endometriosis located elsewhere, a mass involving the round ligament is depicted as T2-hypointense thickening or nodularity with enhancement on contrast-enhanced T1-weighted MR images (Fig 10). Endometriosis reportedly affects the right round ligament more commonly than the left; one hypothesis offered to explain this difference is that the presence of the sigmoid colon prevents retrograde implantation of endometrial glands and stroma onto the left-sided ligament (76).

Endometrial Implants in Scars from Cesarean Section and Laparoscopy

Women may present with palpable masses within laparoscopy incisions or cesarean delivery scars. Symptoms may vary with postpartum menstrual cycles (84). The occurrence of solid endometriosis in these locations is hypothesized to be independent of retrograde menstruation. Direct implantation of endometrial glands and stroma during cesarean delivery or a laparoscopic procedure (typically a myomectomy) is thought to be the cause. In one surgical case series involving 40 women with solid endometriosis of the abdominal wall, the presence of endometriosis was known preoperatively in fewer than half of the women (85). At MR imaging, these masses appear similar to solid endometriosis at other sites (76,86,87). Detection of ectopic endometrial glands should help establish the diagnosis of solid endometriosis and exclude the diagnosis of a desmoid tumor (87), a lesion that is often considered in the differential diagnosis of symptomatic abdominal wall masses in premenopausal women who have undergone cesarean delivery or another abdominal surgical procedure.

Pearl 10: Solid Invasive Endometriosis of the Posterior Uterus Can Mimic Posterior Segmental Adenomyosis

One of the most commonly encountered locations of solid invasive endometriosis is the rectouterine pouch, or posterior cul-de-sac. Solid endometriosis in this site often extends to or invades the posterior myometrium (Figs 1, 3). Solid invasive endometriosis in this location has been labeled "focal intramyometrial adenomyosis" (40) and "subserosal adenomyosis-like lesion" (88). We prefer the term *solid invasive endometriosis* or *deep infiltrative endometriosis of the posterior uterus*. Adenomyosis is not simply defined by the presence of ectopic endometrial glands and stroma outside the endometrial complex and inside the uterus; it arises from abnormalities of the interface between the endometrium and the subjacent myometrium (89,90). Thus, adenomyosis is an "inside-out" process. Solid implants of endometriosis that extend into the posterior myometrium appear similar to adenomyosis when viewed in isolation at imaging. However, solid invasive endometriosis that involves the uterus is an "outside-in" process that often spares the uterine junctional zone, and it should not be misclassified as adenomyosis.

Summary

Endometriosis is a common condition with major and often devastating consequences to the patient. Laparoscopy, which allows visualization only of superficial endometriosis, is complemented by pelvic MR imaging performed with T1 weighting and fat suppression to provide a comprehensive evaluation of disease extension. The 10 pearls of MR imaging of endometriosis that are described and illustrated in this article will help radiologists detect endometriomas, dilated fallopian tubes containing either simple fluid or hemorrhagic content, thickened round and uterosacral ligaments, and solid masses of infiltrating endometriosis located in the posterior

Teaching Point

bladder, posterior uterus, anterior rectosigmoid colon, and surgical scars. These pearls address appropriate MR imaging techniques to differentiate endometriomas from mature cystic teratomas and to indicate when malignant degeneration should be considered. Suggestions for improving the detection of solid endometriosis throughout the pelvis, in cesarean delivery scars, and within the uterus are also offered.

References

1. Luciano DE, Luciano AA. Management of endometriosis-related pain: an update. Womens Health (Lond Engl) 2011;7(5):585–590.
2. Sampson JA. Peritoneal endometriosis due to menstrual dissemination of endometrial tissue into the peritoneal cavity. Am J Obstet Gynecol 1927;14: 422–469.
3. Jensen JR, Coddington CC 3rd. Evolving spectrum: the pathogenesis of endometriosis. Clin Obstet Gynecol 2010;53(2):379–388.
4. Hsu AL, Khachikyan I, Stratton P. Invasive and noninvasive methods for the diagnosis of endometriosis. Clin Obstet Gynecol 2010;53(2):413–419.
5. Coccia ME, Rizzello F. Ultrasonographic staging: a new staging system for deep endometriosis. Ann N Y Acad Sci 2011;1221:61–69.
6. Bulun SE. Endometriosis. N Engl J Med 2009;360 (3):268–279.
7. Brosens I, Puttemans P, Campo R, Gordts S, Kinkel K. Diagnosis of endometriosis: pelvic endoscopy and imaging techniques. Best Pract Res Clin Obstet Gynaecol 2004;18(2):285–303.
8. Ascher SM, Agrawal R, Bis KG, et al. Endometriosis: appearance and detection with conventional and contrast-enhanced fat-suppressed spin-echo techniques. J Magn Reson Imaging 1995;5(3):251–257.
9. Outwater E, Schiebler ML, Owen RS, Schnall MD. Characterization of hemorrhagic adnexal lesions with MR imaging: blinded reader study. Radiology 1993;186(2):489–494.
10. de Ziegler D, Borghese B, Chapron C. Endometriosis and infertility: pathophysiology and management. Lancet 2010;376(9742):730–738.
11. Giudice LC. Clinical practice: endometriosis. N Engl J Med 2010;362(25):2389–2398.
12. Coutinho A Jr, Bittencourt LK, Pires CE, et al. MR imaging in deep pelvic endometriosis: a pictorial essay. RadioGraphics 2011;31(2):549–567.
13. Del Frate C, Girometti R, Pittino M, Del Frate G, Bazzocchi M, Zuiani C. Deep retroperitoneal pelvic endometriosis: MR imaging appearance with laparoscopic correlation. RadioGraphics 2006;26(6): 1705–1718.
14. Bis KG, Vrachliotis TG, Agrawal R, Shetty AN, Maximovich A, Hricak H. Pelvic endometriosis: MR imaging spectrum with laparoscopic correlation and diagnostic pitfalls. RadioGraphics 1997;17(3): 639–655.
15. Takeuchi M, Matsuzaki K, Uehara H, Nishitani H. Malignant transformation of pelvic endometriosis: MR imaging findings and pathologic correlation. RadioGraphics 2006;26(2):407–417.
16. Kuligowska E, Deeds L 3rd, Lu K 3rd. Pelvic pain: overlooked and underdiagnosed gynecologic conditions. RadioGraphics 2005;25(1):3–20.
17. Chamié LP, Blasbalg R, Pereira RM, Warmbrand G, Serafini PC. Findings of pelvic endometriosis at transvaginal US, MR imaging, and laparoscopy. RadioGraphics 2011;31(4):E77–E100.
18. Rezvani M, Shaaban AM. Fallopian tube disease in the nonpregnant patient. RadioGraphics 2011;31 (2):527–548.
19. Woodward PJ, Sohaey R, Mezzetti TP Jr. Endometriosis: radiologic-pathologic correlation. RadioGraphics 2001;21(1):193–216, 288–294.
20. Kim MY, Rha SE, Oh SN, et al. MR imaging findings of hydrosalpinx: a comprehensive review. RadioGraphics 2009;29(2):495–507.
21. Togashi K, Nishimura K, Kimura I, et al. Endometrial cysts: diagnosis with MR imaging. Radiology 1991;180(1):73–78.
22. Glastonbury CM. The shading sign. Radiology 2002;224(1):199–201.
23. Outwater EK, Siegelman ES, Hunt JL. Ovarian teratomas: tumor types and imaging characteristics. RadioGraphics 2001;21(2):475–490.
24. Pereira JM, Sirlin CB, Pinto PS, Casola G. CT and MR imaging of extrahepatic fatty masses of the abdomen and pelvis: techniques, diagnosis, differential diagnosis, and pitfalls. RadioGraphics 2005;25 (1):69–85.
25. Bazot M, Boudghéne F, Billiéres P, Antoine J, Uzan S, Bigot J. Value of fat-suppression gradient-echo MR imaging in the diagnosis of ovarian cystic teratomas. Clin Imaging 2000;24(3):146–153.
26. Stevens SK, Hricak H, Campos Z. Teratomas versus cystic hemorrhagic adnexal lesions: differentiation with proton-selective fat-saturation MR imaging. Radiology 1993;186(2):481–488.
27. Siegelman ES, Outwater EK. Tissue characterization in the female pelvis by means of MR imaging. Radiology 1999;212(1):5–18.
28. Bydder GM, Hajnal JV, Young IR. MRI: use of the inversion recovery pulse sequence. Clin Radiol 1998;53(3):159–176.
29. Krinsky G, Rofsky NM, Weinreb JC. Nonspecificity of short inversion time inversion recovery (STIR) as a technique of fat suppression: pitfalls in image interpretation. AJR Am J Roentgenol 1996;166(3): 523–526.
30. Coutinho AC Jr, Krishnaraj A, Pires CE, Bittencourt LK, Guimarães AR. Pelvic applications of diffusion magnetic resonance images. Magn Reson Imaging Clin N Am 2011;19(1):133–157.

31. Qayyum A. Diffusion-weighted imaging in the abdomen and pelvis: concepts and applications. RadioGraphics 2009;29(6):1797–1810.

32. Whittaker CS, Coady A, Culver L, Rustin G, Padwick M, Padhani AR. Diffusion-weighted MR imaging of female pelvic tumors: a pictorial review. RadioGraphics 2009;29(3):759–774; discussion 774–778.

33. Feuerlein S, Pauls S, Juchems MS, et al. Pitfalls in abdominal diffusion-weighted imaging: how predictive is restricted water diffusion for malignancy. AJR Am J Roentgenol 2009;193(4):1070–1076.

34. Busard MP, Mijatovic V, van Kuijk C, Pieters-van den Bos IC, Hompes PG, van Waesberghe JH. Magnetic resonance imaging in the evaluation of (deep infiltrating) endometriosis: the value of diffusion-weighted imaging. J Magn Reson Imaging 2010;32 (4):1003–1009.

35. Nakayama T, Yoshimitsu K, Irie H, et al. Diffusion-weighted echo-planar MR imaging and ADC mapping in the differential diagnosis of ovarian cystic masses: usefulness of detecting keratinoid substances in mature cystic teratomas. J Magn Reson Imaging 2005;22(2):271–278.

36. Silvera S, Oppenheim C, Touzé E, et al. Spontaneous intracerebral hematoma on diffusion-weighted images: influence of T2-shine-through and T2-blackout effects. AJNR Am J Neuroradiol 2005;26 (2):236–241.

37. Namimoto T, Awai K, Nakaura T, Yanaga Y, Hirai T, Yamashita Y. Role of diffusion-weighted imaging in the diagnosis of gynecological diseases. Eur Radiol 2009;19(3):745–760.

38. Outwater EK, Siegelman ES, Chiowanich P, Kilger AM, Dunton CJ, Talerman A. Dilated fallopian tubes: MR imaging characteristics. Radiology 1998; 208(2):463–469.

39. Gougoutas CA, Siegelman ES, Hunt J, Outwater EK. Pelvic endometriosis: various manifestations and MR imaging findings. AJR Am J Roentgenol 2000;175(2):353–358.

40. Bennett GL, Slywotzky CM, Cantera M, Hecht EM. Unusual manifestations and complications of endometriosis—spectrum of imaging findings: pictorial review. AJR Am J Roentgenol 2010;194(6 suppl):WS34–WS46.

41. Rock JA, Zacur HA, Dlugi AM, Jones HW Jr, TeLinde RW. Pregnancy success following surgical correction of imperforate hymen and complete transverse vaginal septum. Obstet Gynecol 1982;59(4): 448–451.

42. Uğur M, Turan C, Mungan T, et al. Endometriosis in association with müllerian anomalies. Gynecol Obstet Invest 1995;40(4):261–264.

43. Reinhold C, Hricak H, Forstner R, et al. Primary amenorrhea: evaluation with MR imaging. Radiology 1997;203(2):383–390.

44. Junqueira BL, Allen LM, Spitzer RF, Lucco KL, Babyn PS, Doria AS. Müllerian duct anomalies and mimics in children and adolescents: correlative intraoperative assessment with clinical imaging. RadioGraphics 2009;29(4):1085–1103.

45. Saleem SN. MR imaging diagnosis of uterovaginal anomalies: current state of the art. RadioGraphics 2003;23(5):e13.

46. Iwamoto H, Suzuki M, Watanabe N, Minai M, Hirata S, Hoshi K. Case study of a pregnant woman with decidualized ovarian endometriosis whose preoperative findings suggested malignant transformation. Eur J Gynaecol Oncol 2006;27(3):301–303.

47. Miyakoshi K, Tanaka M, Gabionza D, et al. Decidualized ovarian endometriosis mimicking malignancy. AJR Am J Roentgenol 1998;171(6):1625–1626.

48. Sammour RN, Leibovitz Z, Shapiro I, et al. Decidualization of ovarian endometriosis during pregnancy mimicking malignancy. J Ultrasound Med 2005;24 (9):1289–1294.

49. Yoshida S, Onogi A, Shigetomi H, et al. Two cases of pregnant women with ovarian endometrioma mimicking a malignant ovarian tumor. J Clin Ultrasound 2008;36(8):512–516.

50. Machida S, Matsubara S, Ohwada M, et al. Decidualization of ovarian endometriosis during pregnancy mimicking malignancy: report of three cases with a literature review. Gynecol Obstet Invest 2008;66(4): 241–247.

51. Barbieri M, Somigliana E, Oneda S, Ossola MW, Acaia B, Fedele L. Decidualized ovarian endometriosis in pregnancy: a challenging diagnostic entity. Hum Reprod 2009;24(8):1818–1824.

52. Takeuchi M, Matsuzaki K, Nishitani H. Magnetic resonance manifestations of decidualized endometriomas during pregnancy. J Comput Assist Tomogr 2008;32(3):353–355.

53. Van Gorp T, Amant F, Neven P, Vergote I, Moerman P. Endometriosis and the development of malignant tumours of the pelvis: a review of literature. Best Pract Res Clin Obstet Gynaecol 2004;18(2): 349–371.

54. Kumar S, Munkarah A, Arabi H, et al. Prognostic analysis of ovarian cancer associated with endometriosis. Am J Obstet Gynecol 2011;204(1):63.e1–e7.

55. Erzen M, Rakar S, Klancnik B, Syrjänen K. Endometriosis-associated ovarian carcinoma (EAOC): an entity distinct from other ovarian carcinomas as suggested by a nested case-control study. Gynecol Oncol 2001;83(1):100–108.

56. Patrelli TS, Berretta R, Gizzo S, et al. CA 125 serum values in surgically treated endometriosis patients and its relationships with anatomic sites of endometriosis and pregnancy rate. Fertil Steril 2011;95(1): 393–396.

57. Huhtinen K, Suvitie P, Hiissa J, et al. Serum HE4 concentration differentiates malignant ovarian tumours from ovarian endometriotic cysts. Br J Cancer 2009;100(8):1315–1319.

58. Montagnana M, Lippi G, Danese E, Franchi M, Guidi GC. Usefulness of serum HE4 in endometriotic cysts. Br J Cancer 2009;101(3):548.

59. Tanaka YO, Yoshizako T, Nishida M, Yamaguchi M, Sugimura K, Itai Y. Ovarian carcinoma in patients with endometriosis: MR imaging findings. AJR Am J Roentgenol 2000;175(5):1423–1430.

60. McDermott S, Oei TN, Iyer VR, Lee SI. MR imaging of malignancies arising in endometriomas and extraovarian endometriosis. RadioGraphics 2012;32 (3):845–863.

61. Hecht EM, Israel GM, Krinsky GA, et al. Renal masses: quantitative analysis of enhancement with signal intensity measurements versus qualitative analysis of enhancement with image subtraction for diagnosing malignancy at MR imaging. Radiology 2004;232(2):373–378.

62. Siegelman ES, Outwater E, Wang T, Mitchell DG. Solid pelvic masses caused by endometriosis: MR imaging features. AJR Am J Roentgenol 1994;163 (2):357–361.

63. Bazot M, Gasner A, Ballester M, Daraï E. Value of thin-section oblique axial T2-weighted magnetic resonance images to assess uterosacral ligament endometriosis. Hum Reprod 2011;26(2):346–353.

64. Reinhold C, Tafazoli F, Mehio A, et al. Uterine adenomyosis: endovaginal US and MR imaging features with histopathologic correlation. RadioGraphics 1999;19(Spec Issue):S147–S160.

65. Jenkins S, Olive DL, Haney AF. Endometriosis: pathogenetic implications of the anatomic distribution. Obstet Gynecol 1986;67(3):335–338.

66. Grasso RF, Di Giacomo V, Sedati P, et al. Diagnosis of deep infiltrating endometriosis: accuracy of magnetic resonance imaging and transvaginal 3D ultrasonography. Abdom Imaging 2010;35(6):716–725.

67. Bazot M, Lafont C, Rouzier R, Roseau G, Thomassin-Naggara I, Daraï E. Diagnostic accuracy of physical examination, transvaginal sonography, rectal endoscopic sonography, and magnetic resonance imaging to diagnose deep infiltrating endometriosis. Fertil Steril 2009;92(6):1825–1833.

68. Loubeyre P, Petignat P, Jacob S, Egger JF, Dubuisson JB, Wenger JM. Anatomic distribution of posterior deeply infiltrating endometriosis on MRI after vaginal and rectal gel opacification. AJR Am J Roentgenol 2009;192(6):1625–1631.

69. Caramella T, Novellas S, Fournol M, et al. Deep pelvic endometriosis: MRI features [in French]. J Radiol 2008;89(4):473–479.

70. Chassang M, Novellas S, Bloch-Marcotte C, et al. Utility of vaginal and rectal contrast medium in MRI for the detection of deep pelvic endometriosis. Eur Radiol 2010;20(4):1003–1010.

71. Roman H, Vassilieff M, Gourcerol G, et al. Surgical management of deep infiltrating endometriosis of the rectum: pleading for a symptom-guided approach. Hum Reprod 2011;26(2):274–281.

72. Dousset B, Leconte M, Borghese B, et al. Complete surgery for low rectal endometriosis: long-term results of a 100-case prospective study. Ann Surg 2010;251(5):887–895.

73. Abrão MS, Podgaec S, Dias JA Jr, Averbach M, Silva LF, Marino de Carvalho F. Endometriosis lesions that compromise the rectum deeper than the inner muscularis layer have more than 40% of the circumference of the rectum affected by the disease. J Minim Invasive Gynecol 2008;15(3):280–285.

74. Yoon JH, Choi D, Jang KT, et al. Deep rectosigmoid endometriosis: "mushroom cap" sign on T2-weighted MR imaging. Abdom Imaging 2010;35(6):726–731.

75. Vercellini P, Frontino G, Pisacreta A, De Giorgi O, Cattaneo M, Crosignani PG. The pathogenesis of bladder detrusor endometriosis. Am J Obstet Gynecol 2002;187(3):538–542.

76. Novellas S, Chassang M, Bouaziz J, Delotte J, Toullalan O, Chevallier EP. Anterior pelvic endometriosis: MRI features. Abdom Imaging 2010;35(6):742–749.

77. Wong-You-Cheong JJ, Woodward PJ, Manning MA, Davis CJ. Inflammatory and nonneoplastic bladder masses: radiologic-pathologic correlation. RadioGraphics 2006;26(6):1847–1868.

78. Tokue H, Tsushima Y, Endo K. Magnetic resonance imaging findings of extrapelvic endometriosis of the round ligament. Jpn J Radiol 2009;27(1):45–47.

79. Hagiwara Y, Hatori M, Moriya T, et al. Inguinal endometriosis attaching to the round ligament. Australas Radiol 2007;51(1):91–94.

80. Cervini P, Mahoney J, Wu L. Endometriosis in the canal of Nuck: atypical manifestations in an unusual location. AJR Am J Roentgenol 2005;185(1):284–285.

81. Kirkpatrick A, Reed CM, Bui-Mansfield LT, Russell MJ, Whitford W. Radiologic-pathologic conference of Brooke Army Medical Center: endometriosis of the canal of Nuck. AJR Am J Roentgenol 2006;186 (1):56–57.

82. Gaeta M, Minutoli F, Mileto A, et al. Nuck canal endometriosis: MR imaging findings and clinical features. Abdom Imaging 2010;35(6):737–741.

83. Crispi CP, de Souza CA, Oliveira MA, et al. Endometriosis of the round ligament of the uterus. J Minim Invasive Gynecol 2012;19(1):46–51.

84. Hensen JH, Van Breda Vriesman AC, Puylaert JB. Abdominal wall endometriosis: clinical presentation and imaging features with emphasis on sonography. AJR Am J Roentgenol 2006;186(3):616–620.

85. Bektaş H, Bilsel Y, Sari YS, et al. Abdominal wall endometrioma: a 10-year experience and brief review of the literature. J Surg Res 2010;164(1):e77–e81.

86. Busard MP, Mijatovic V, van Kuijk C, Hompes PG, van Waesberghe JH. Appearance of abdominal wall endometriosis on MR imaging. Eur Radiol 2010;20 (5):1267–1276.

87. Muto MG, O'Neill MJ, Oliva E. A 45-year-old woman with a painful mass in the abdomen, case 18-2005. N Engl J Med 2005;352(24):2535–2542.

88. Takeuchi M, Matsuzaki K. Adenomyosis: usual and unusual imaging manifestations, pitfalls, and problem-solving MR imaging techniques. RadioGraphics 2011;31(1):99–115.

89. Gordts S, Brosens JJ, Fusi L, Benagiano G, Brosens I. Uterine adenomyosis: a need for uniform terminology and consensus classification. Reprod Biomed Online 2008;17(2):244–248.

90. Novellas S, Chassang M, Delotte J, et al. MRI characteristics of the uterine junctional zone: from normal to the diagnosis of adenomyosis. AJR Am J Roentgenol 2011;196(5):1206–1213.

MR Imaging of Endometriosis: Ten Imaging Pearls

Evan S. Siegelman, MD • Edward R. Oliver, MD, PhD

Page 1678

[W]e recommend that all MR imaging examinations of the female pelvis include a T1-weighted fat-suppressed sequence for two reasons: First, the loss of signal intensity within a T1-hyperintense adnexal mass at fat-suppressed imaging facilitates characterization of the mass as a mature cystic teratoma (23–27). Second, saturation of the high signal intensity of fat improves the dynamic range of T1-weighted images by enhancing the differences among non–fat-containing T1-hyperintense structures, thereby enabling more sensitive detection of smaller endometriomas (Figs 1b, 2c, 3b).

Page 1680

The presence of T1-weighted hyperintensity within a dilated fallopian tube is suggestive of endometriosis (Fig 1) and may be the only finding at MR imaging in some women (38).

Page 1682

Decidualized endometriosis has been described as a mimic of ovarian cancer at ultrasonography (US) and MR imaging (46–50).

Page 1684

Although most endometriomas are easily recognized on the basis of their T1 hyperintensity, solid masses of endometriosis can easily be overlooked.

Page 1688

One of the most commonly encountered locations of solid invasive endometriosis is the rectouterine pouch, or posterior cul-de-sac. Solid endometriosis in this site often extends to or invades the posterior myometrium (Figs 1, 3).